

Positronium formation into arbitrary excited states in e^+ -H scattering

B. C. Saha

Department of Physics & Astronomy, The University of Oklahoma, Norman, Oklahoma 73019

P. K. Roy

Department of Physics, Darjeeling Government College, Darjeeling 734101, West Bengal, India

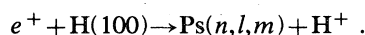
(Received 5 March 1984)

The rearrangement collision problem of positronium formation into arbitrary n, l, m states by positrons from hydrogen atoms in the ground state has been investigated employing the first Born approximation and the first-order exchange approximation. It is shown that for fixed l, m , n^3 times the asymptotic cross section, if multiplied by the factor $\prod_{\alpha=0}^l (1 - \alpha^2 n^{-2})$, gives a good estimate of the n^3 cross section of the corresponding n, l, m state when n is not too low. For s state the first-order-exchange-approximation results are greater than those of the first Born approximation. The momentum-transfer cross sections in the first Born approximation overestimate the first-order-exchange-approximation results throughout the energy range considered.

I. INTRODUCTION

Recent discoveries of the 0.51-MeV positron annihilation gamma rays coming from¹ solar flares and from² the direction of the center of our galaxy have led to a considerable interest in the problem of positron-atom collisions.³ A knowledge of the cross sections of positronium (Ps) formation in the positron-hydrogen-atom collision may provide much information regarding the environment at the site of the origin of these gamma rays. Direct measurements⁴ of the cross section for Ps formation into excited states have now become possible with the development of more advanced technology.

In the present work we intend to study the following rearrangement collision process:



In view of the practical difficulties in carrying out sophisticated calculations for the Ps formation into highly excited states we here employ the first Born approximation (FBA). In addition, we also present results in the first-order exchange approximation⁵ (FOEA) which is an improvement over the FBA in that all terms of the first order in the interaction potential as obtained from the two-state approximation are retained in the expression of the scattering amplitude.

It is well known that the FBA does not take into account the effect of the lack of orthogonality of the initial and final bound-state wave functions. The FOEA, on the other hand, makes allowance of this nonorthogonality of the wave functions and thus leads to a more consistent treatment of the scattering process.

The organization of the paper is as follows. In Sec. II we give the general expressions of the scattering amplitudes for Ps formation into an arbitrary n, l, m state in the FBA and FOEA. In Sec. III we discuss the reduction of the integrals occurring in the expressions of the scattering amplitude. In Sec. IV we consider the case when $n \rightarrow \infty$.

We present our results in Sec. V and make our concluding remarks in Sec. VI. Unless otherwise noted, we use atomic units throughout our discussion.

II. THEORY

Let \vec{r}_1 and \vec{r}_2 respectively denote the position vectors of the incident positron and the target electron relative to the proton which is assumed to be infinitely heavy and situated at the origin of the coordinate system. The positron on collision captures the target electron to form a bound state (positronium) in the final channel.

The time-independent Schrödinger equation is

$$(H - E)\Psi = 0. \quad (1)$$

The Hamiltonian H of the system can be expressed in either of the two forms:

$$H = -\frac{1}{2\mu_i} \nabla_{r_1}^2 - \frac{1}{2a} \nabla_{r_2}^2 - \frac{1}{r_2} - \frac{1}{x} + \frac{1}{r_1} \quad (2a)$$

$$= -\frac{1}{2\mu_f} \nabla_{\rho}^2 - \frac{1}{2b} \nabla_x^2 - \frac{1}{r_2} - \frac{1}{x} + \frac{1}{r_1}. \quad (2b)$$

In the above expression μ_i, μ_f are the reduced masses of the system in the initial and the final channel; $\mu_i = 1$ and $\mu_f = 2$. We define the vectors $\vec{\rho}$ and \vec{x} by $\vec{\rho} = (\vec{r}_1 + \vec{r}_2)/2$ and $\vec{x} = \vec{r}_2 - \vec{r}_1$. The reduced masses a and b in the initial and final bound systems are 1 and $\frac{1}{2}$, respectively.

The initial and the final bound-state wave functions satisfy the following equations:

$$\left[-\frac{1}{2a} \nabla_{r_2}^2 - \frac{1}{r_2} \right] \psi(\vec{r}_2) = \epsilon_i \psi(\vec{r}_2), \quad (3a)$$

$$\left[-\frac{1}{2b} \nabla_x^2 - \frac{1}{x} \right] \phi(\vec{x}) = \epsilon_f \phi(\vec{x}), \quad (3b)$$

where ϵ_i and ϵ_f are the eigenenergies of the initial hydrogen atom and the final positronium atom, respectively.

In the two-state approximation the total wave function Ψ can be expanded as

$$\Psi = \psi(\vec{r}_2)F(\vec{r}_1) + \phi(\vec{x})G(\vec{\rho}). \quad (4)$$

As usual the total energy is given by

$$E = \frac{1}{2\mu_i}K_i^2 + \epsilon_i \quad (5a)$$

$$= \frac{1}{2\mu_f}K_f^2 + \epsilon_f, \quad (5b)$$

where \vec{K}_i and \vec{K}_f denote, respectively, the initial and final momenta.

In order to obtain the transition matrix element, the trial wave function in Eq. (4) is substituted in Eq. (1). Then multiplying both sides of the resulting equation by $\psi^*(\vec{r}_2)$ and performing the integration over \vec{r}_2 we obtain, employing Eqs. (2a), (3a), and (5a),

$$\begin{aligned} (\nabla_{r_1}^2 + K_i^2)F(\vec{r}_1) &= 2\mu_i \int \psi^*(\vec{r}_2) \left[\frac{1}{r_1} - \frac{1}{x} \right] \psi(\vec{r}_2)F(\vec{r}_1) d\vec{r}_2 \\ &+ 2\mu_f \int \psi^*(\vec{r}_2)(H-E)\phi(\vec{x})G(\vec{\rho}) d\vec{r}_2. \end{aligned} \quad (6)$$

On multiplying by $\phi^*(\vec{x})$ and integrating over \vec{x} we may obtain in the same way the equation for $G(\vec{\rho})$ as

$$\begin{aligned} (\nabla_{\rho}^2 + K_f^2)G(\vec{\rho}) &= 2\mu_f \int \phi^*(\vec{x}) \left[\frac{1}{r_1} - \frac{1}{r_2} \right] \phi(\vec{x})G(\vec{\rho}) d\vec{x} \\ &+ 2\mu_f \int \phi^*(\vec{x})(H-E)\psi(\vec{r}_2)F(\vec{r}_1) d\vec{x}. \end{aligned} \quad (7)$$

Equation (7) gets further simplified if one neglects the self-coupling altogether. In such a case $G(\vec{\rho})$ satisfies the equation

$$(\nabla_{\rho}^2 + K_f^2)G(\vec{\rho}) = 2\mu_f \int \phi^*(\vec{x})(H-E)\psi(\vec{r}_2)F(\vec{r}_1) d\vec{x}. \quad (8)$$

Using Green's-function technique the transition amplitude is then obtained as

$$\begin{aligned} g(\theta) &= -\frac{\mu_f}{2\pi} \int \exp(-i\vec{K}_f \cdot \vec{\rho}) \phi^*(\vec{x}) \\ &\times (H-E)\psi(\vec{r}_2)F(\vec{r}_1) d\vec{x} d\vec{\rho}, \end{aligned} \quad (9)$$

where $\theta [= \cos^{-1}(\hat{K}_i \cdot \hat{K}_f)]$ is the scattering angle. Since in the above expression $F(\vec{r}_1)$ is not known exactly, some suitable approximate form for $F(\vec{r}_1)$ is chosen for the calculation of the scattering section.

The differential cross section (DCS) is obtained from the relation

$$\frac{d\sigma}{d\Omega} = \frac{K_f}{K_i} |g(\theta)|^2. \quad (10)$$

The total cross section (TCS) is evaluated by integrating the above expression over the entire solid angle. The momentum-transfer cross section (MTCS) may be calculated from the differential cross section by the relation

$$\sigma^{\text{MT}(i \rightarrow f)} = \int_{\Omega} \frac{d\sigma}{d\Omega} \left[1 - \frac{K_f}{K_i} \cos\theta \right] d\Omega. \quad (11)$$

Several approximation methods have been developed in order to calculate $g(\theta)$ in Eq. (9), the simplest of which results from the first Born approximation.

A. FBA

In the FBA, $F(\vec{r}_1)$ is approximated by the plane wave $\exp(i\vec{K}_i \cdot \vec{r}_1)$. Equation (9) thus takes the form

$$\begin{aligned} g^{\text{FBA}}(\theta) &= -\frac{\mu_f}{2\pi} \int \exp(-i\vec{K}_f \cdot \vec{\rho} + i\vec{K}_i \cdot \vec{r}_1) \phi^*(\vec{x}) \\ &\times V_{\text{int}}\psi(\vec{r}_2) d\vec{x} d\vec{\rho}, \end{aligned} \quad (12)$$

where the interaction potential V_{int} may be taken either as V_i , the prior interaction or as V_f , the post interaction:

$$V_i = \frac{1}{r_1} - \frac{1}{x}, \quad (13a)$$

$$V_f = \frac{1}{r_1} - \frac{1}{r_2}. \quad (13b)$$

In the present case the bound-state wave functions being exact there is, however, no "post-prior" discrepancy. Substituting (13a) into Eq. (12) we get

$$g^{\text{FBA}}(\theta) = -\frac{\mu_f}{2\pi} (I + J), \quad (14)$$

where

$$I = \int x^{-1} \exp[i(\vec{\alpha} \cdot \vec{r}_2 - \vec{\beta} \cdot \vec{x})] \phi^*(\vec{x}) \psi(\vec{r}_2) d\vec{x} d\vec{r}_2 \quad (15)$$

and

$$J = - \int r_1^{-1} \exp[i(\vec{\alpha} \cdot \vec{r}_2 - \vec{\beta} \cdot \vec{x})] \phi^*(\vec{x}) \psi(\vec{r}_2) d\vec{x} d\vec{r}_2 \quad (16)$$

with

$$\vec{\alpha} = \mu_i \vec{K}_i - \vec{K}_f, \quad \vec{\beta} = \vec{K}_i - \mu_f \vec{K}_f.$$

It may be noted that the initial- and the final-state wave functions, $\psi(\vec{r}_2)$ and $\phi(\vec{x})$, occurring in Eq. (12) are not orthogonal. Consequently, a constant term when added to the interaction potential V_{int} gives a nonvanishing contribution to the scattering amplitude which is rather unphysical. This undesirable feature of the FBA is rectified in the first-order exchange approximation (FOEA).

B. FOEA

The FOEA is an attempt to improve upon the FBA by retaining terms of the first order in the interaction potential occurring in the two-state coupled equations. It is clearly seen from the Eq. (9) that if we substitute $F(\vec{r}_1) = \exp(i\vec{K}_i \cdot \vec{r}_1)$ in the right-hand side of Eq. (9) then $(\nabla_{r_1}^2 + K_i^2)F(\vec{r}_1)$ has a vanishing contribution to $g(\theta)$.

However, from Eq. (6) it is evident that this term should contribute to the scattering amplitude. To take account of the contribution of $(\nabla_{\vec{r}_1}^2 + K_i^2)F(\vec{r}_1)$ to the scattering amplitude we use, in the FOEA, Eq. (6) retaining only terms up to the first order in the interaction potential. Thus we use

$$(\nabla_{\vec{r}_1}^2 + K_i^2)F(\vec{r}_1) = 2\mu_i \int d\vec{r}_2 \psi^*(\vec{r}_2) V_i \psi(\vec{r}_2) \exp(i\vec{K}_i \cdot \vec{r}_1). \quad (17)$$

The FOEA amplitude takes the form

$$g^{\text{FOEA}}(\theta) = -\frac{\mu_f}{2\pi} \int \exp(-i\vec{K}_f \cdot \vec{\rho} + i\vec{K}_i \cdot \vec{r}_1) \phi^*(\vec{x}) \times V_D \psi(\vec{r}_2) d\vec{x} d\vec{\rho}, \quad (18)$$

where the distorting potential V_D is given by

$$V_D = V_i - U_i.$$

U_i is the average of the interaction potential V_i over the initial bound state, i.e.,

$$U_i = \int \psi^*(\vec{r}') V_i \psi(\vec{r}') d\vec{r}'. \quad (19)$$

The scattering amplitude in this case reads as

$$g^{\text{FOEA}}(\theta) = -\frac{\mu_f}{2\pi} (I + J + \mathcal{X}) = g^{\text{FBA}}(\theta) + \frac{\mu_f}{2\pi} \mathcal{X}, \quad (20)$$

where the new integral \mathcal{X} takes form

$$\mathcal{X} = \int \exp(-i\vec{K}_f \cdot \vec{\rho} + i\vec{K}_i \cdot \vec{r}_1) \phi^*(\vec{x}) U_i \psi(\vec{r}_2) d\vec{x} d\vec{\rho}. \quad (21)$$

In order to evaluate the Ps-formation cross section in the FOEA we use Eq. (20) which is similar to that first derived by Feenberg⁵ in the case of e^- -H collision. The expression of the e^- -H scattering amplitude as obtained by Bell and Moisewitsch⁶ using a variational principle contains some additional terms; their contribution is, however, negligible.⁷

III. REDUCTION OF THE AMPLITUDE

The initial and the final bound-state wave functions are given by

$$\psi(\vec{r}) = \psi_{100}(\vec{r}) = \left[\frac{\gamma_1^3}{\pi} \right]^{1/2} \exp(-\gamma_1 r), \quad \gamma_1 = 1 \quad (22a)$$

and

$$\phi(\vec{x}) = \phi_{nlm}(\vec{x}) = N_{nlm} R_{nl}(x) Y_{lm}(\hat{x}), \quad (22b)$$

where

$$R_{nl}(x) = x^l \exp(-\gamma_n x) L_{n+l}^{2l+1}(2\gamma_n x), \quad \gamma_n = \mu_f/n.$$

The normalization constant N_{nlm} is given by

$$N_{nlm} = -\frac{(2\gamma_n)^{l+1}}{(n+l)!} \left[\frac{\gamma_n (n-l-1)!}{n(n+1)!} \right]^{1/2}. \quad (23)$$

$Y_{lm}(\theta, \phi)$ represents the spherical harmonics, and $L_a^b(x)$ is the associated Laguerre polynomial. Instead of using the

series representation of the $L_a^b(x)$ we used a contour-integral representation which reads as

$$L_{n+l}^{2l+1}(x) = -\frac{(n+l)!}{2\pi i} \oint_{\Gamma} dt \frac{\exp[-xt/(1-t)]}{(1-t)^{2l+2} t^{n-l}}. \quad (24)$$

The contour Γ includes the origin but does not enclose the point $t=1$. The integration over \vec{r}_2 and \vec{x} in the integral I can be carried out analytically. The final result, apart from some constant factors, reads as

$$I \sim [(\alpha^2 + \gamma_1^2)(\beta^2 + \gamma_n^2)^{l+2}]^{-1} (2\beta)^l Y_{lm}^*(-\hat{\beta}) C_{n-l-1}^{l+1}(\eta'), \quad (25)$$

where $C_a^b(x)$ represents the Gegenbauer polynomials and $\eta' = (\beta^2 - \gamma_n^2)(\beta^2 + \gamma_n^2)^{-1}$.

The results for the integrals J and \mathcal{X} may be obtained from the auxiliary integral M defined by

$$M = \int r_1^{-1} \exp[i(\vec{\alpha} \cdot \vec{r}_2 - \vec{\beta} \cdot \vec{x}) - y\gamma_1 r_1] \phi^*(\vec{x}) \psi(\vec{r}_2) d\vec{x} d\vec{r}_2 \quad (26)$$

with the help of the relation

$$J = M \Big|_{y=0} \quad (27a)$$

and

$$\mathcal{X} = \left[1 - \frac{d}{dy} \right] M \Big|_{y=2}. \quad (27b)$$

In the integral \mathcal{X} we use the expression for U_i , the static potential of the hydrogen atom, given by

$$U_i = r_1^{-1} (1 + \gamma_1 r_1) \exp(-2\gamma_1 r_1).$$

In order to evaluate the integral M given by Eq. (26), we, however, use the technique outlined by Roy *et al.*⁸ to obtain

$$M \sim \frac{d}{d\gamma_1} \int_0^1 \frac{dz}{\omega} (2\mathcal{S})^l Y_{lm}^*(\hat{\mathcal{S}}) \times \left[\frac{d\Delta}{d\omega} C_{n-l-1}^{l+1}(\eta) + \Delta(2l+1) C_{n-l-2}^{l+2}(\eta) \frac{d\eta}{d\omega} \right], \quad (28)$$

where

$$\hat{\mathcal{S}} = \vec{\alpha}(1-z) - \vec{\beta},$$

$$\omega^2 = (\gamma_1^2 + \alpha^2 z)(1-z) + y^2 z,$$

$$\Delta^2 = (\mathcal{S}^2 + a_1^2)^{n-l-1} (\mathcal{S}^2 + a_2^2)^{-n-l-1},$$

$$a_1 = \gamma_n - \omega, \quad a_2 = \gamma_n + \omega,$$

$$\eta^2 = (\mathcal{S}^2 + \omega^2 - \gamma_n^2)^2 [(\mathcal{S}^2 + a_1^2)(\mathcal{S}^2 + a_2^2)]^{-1}.$$

IV. ASYMPTOTIC ($n \gg 1$) CASE

It has been observed that the Ps-formation cross sections into different angular momentum (l, m) states obey the same scaling law as proposed by Roy *et al.*⁸ in case of

p -H collision. The scaling law enables one to estimate the various cross sections with a knowledge of the asymptotic n^3 cross section for Ps formation.

These asymptotic n^3 cross sections may be found from the limiting values of the integrals when $n \rightarrow \infty$:

$$[S^{-1}I]_{n \rightarrow \infty} = 2C(\gamma_1^2 + \alpha^2)^{-1} \beta^{-(2l+4)} j_l(z_1) Y_{lm}^*(-\beta), \quad (29a)$$

$$\begin{aligned} [S^{-1}M]_{n \rightarrow \infty} &= -C \frac{d}{d\gamma_1} \int_0^1 \frac{dz}{\omega} \mathcal{F}^l z_2^{-l} Y_{lm}^*(\mathcal{F}) \\ &\quad \otimes \left[\frac{d\Delta_1}{d\omega} j_l(z_2) \right. \\ &\quad \left. + \frac{8\Delta_1\omega}{(\mathcal{F}^2 + \omega^2)z_2} j_{l+1}(z_2) \right], \quad (29b) \end{aligned}$$

where

$$S^2 = n^{-3} \prod_{r=0}^l (1 - n^{-2}r^2), \quad (30)$$

$$z_1 = \frac{2}{|\vec{\beta}|}, \quad z_2 = \frac{\sqrt{2}|\vec{\mathcal{F}}|}{(\mathcal{F}^2 + \omega^2)},$$

$$\Delta_1 = (ab)^{-(l+1)} \exp \left[-\frac{2\gamma_1}{\mathcal{F}^2 + \gamma_1^2} \right],$$

$$a = \mathcal{F}^2 + (\gamma_n - \omega)^2,$$

$$b = \mathcal{F}^2 + (\gamma_n + \omega)^2,$$

$$C = 8\pi^{3/2} (i\mu_f)^{l+1}.$$

It may be noted that as $n \rightarrow \infty$, $\gamma_n \rightarrow 0$ and $S^{-1} \rightarrow n^{3/2}$. It is seen that the asymptotic $[n^3 \sigma^{\text{Ps}}]_{n \rightarrow \infty}$ for a particular

angular momentum state if multiplied with $\prod_{\alpha=0}^l (1 - n^{-2}\alpha^2)$ gives a good estimate of the n^3 cross section of the corresponding n, l, m states when the value of the principle quantum numbers n is not too small.

V. RESULTS AND DISCUSSIONS

We have computed results for the differential, total, and momentum-transfer cross sections for the Ps formation into an arbitrary n, l, m state from the ground state of atomic hydrogen. The energy range considered is $E = 20 - 1000$ eV.

For the evaluation of the M integral numerically we use Gaussian quadrature method. Convergence of the result is tested by increasing the mesh points and finally we use 32 quadrature points. The integrated cross sections have also been obtained using the Gaussian quadrature method. We use $\cos\theta$, θ being the scattering angle, as integration variable. As the main contribution to the integrated cross sections comes from the forward direction, we employ a sufficient number of mesh points to get convergent results. We keep 40 quadrature points throughout our calculation. As a check on our general program the FBA values obtained earlier by Sil *et al.*⁹ and the ground-state Ps-formation cross sections in the FOEA of Mandal and Guha¹⁰ have been reproduced.

A. Differential cross sections

Even though the ground-state Ps-formation calculation of Mandal and Guha¹⁰ in the FOEA exists, there is, however, no such calculation on the excited-state Ps formation. The FOEA corrects the problem of nonorthogonality between the initial and final bound state wave functions and it seems to represent an improvement over the FBA. In their study Sil *et al.*⁹ discussed the behavior of the FBA DCS for excited ns and np states while Mandal and

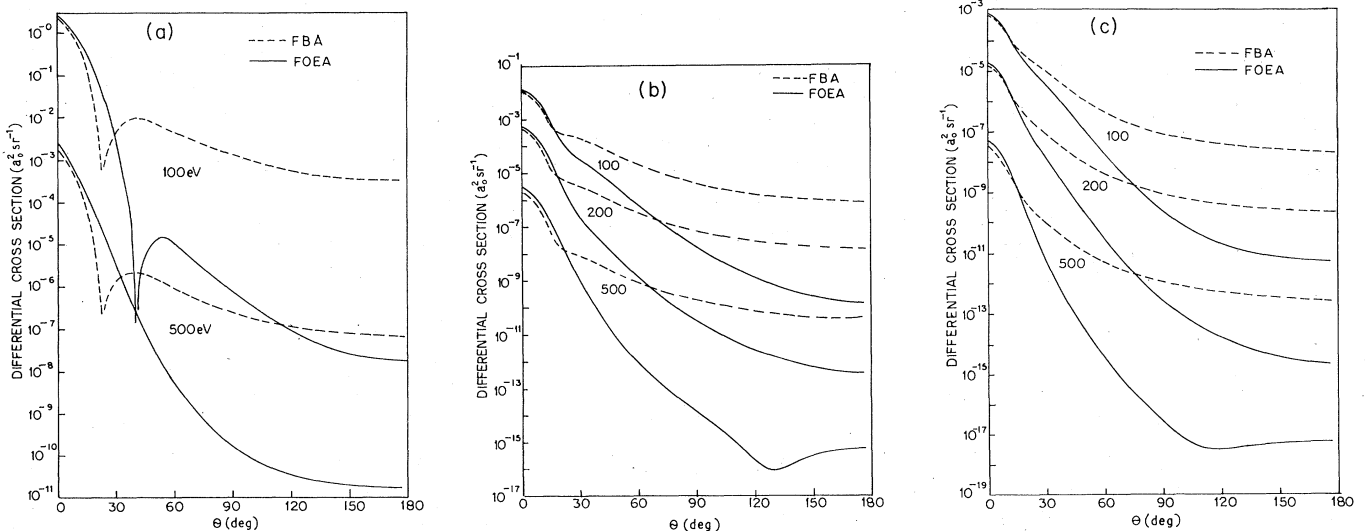


FIG. 1. (a) Differential cross sections $[n^3 d\sigma/d\Omega]_{n \rightarrow \infty}$ in units of a_0^2/sr for Ps formation into excited s states at $E = 100$ and 500 eV. (b) Differential cross sections $[n^3 d\sigma/d\Omega]_{n \rightarrow \infty}$ in units of a_0^2/sr for Ps formation into excited p states at $E = 100, 200,$ and 500 eV. (c) Differential cross sections $[n^3 d\sigma/d\Omega]_{n \rightarrow \infty}$ in units of a_0^2/sr for Ps formation into excited d states at $E = 100, 200,$ and 500 eV.

Guha¹⁰ using FOEA showed the formation cross section only in $1s$ state. Since this is the first application of the FOEA for calculating the excited-state Ps-formation cross sections, it will be useful to compare FBA DCS with their FOEA counterpart for the asymptotic ($n \rightarrow \infty$) states. These are, however, typical results—the DCS for any excited discrete state is qualitatively similar.

In Fig. 1(a) we plot the asymptotic n^3 DCS $[n^3 d\sigma/d\Omega]_{n \rightarrow \infty}$ for Ps formation into the s state at $E=100$ and 500 eV. From Fig. 1(a) it is evident that the FBA DCS exhibits a zero at the scattering angle around 26° for an incident energy of $E=100$ eV. The angular position of the zero moves towards the forward direction as E increases; at $E=500$ eV it is around 22° . It has been observed that the zero position of the angular distribution in the FBA for discrete states remains nearly constant irrespective of the value of the principal quantum number n . On the other hand in the FOEA, the DCS for $E > 200$ eV does not predict any such zero. The same feature has also been earlier noted by Mandal and Guha¹⁰ in their study of Ps formation into the $1s$ state. The origin of this zero in the DCS is due to the mutual cancellation of the contribution of the attractive and repulsive part of the interaction potential. But for $l=1$, as shown in Fig. 1(b), the sum of the contributions of all m -degenerate states produces a kink instead of a zero. This occurs due to the fact that the different m -valued amplitudes show zeros at different scattering angles and their accumulated results yield this kink. This feature is also true for the $l > 1$ states DCS [see Fig. 1(c)] in both the FBA and FOEA. With the increase in positron impact energy the DCS curves fall steadily from a forward peak. Inspection of Fig. 1 reveals that the FBA results, except near the forward direction, lie well above their FOEA counterpart. The large-angle behavior is quite different in that the FOEA results drop off more rapidly than their FBA counterparts. It is interesting to note that the magnitude of the cross section decreases rapidly with increasing l .

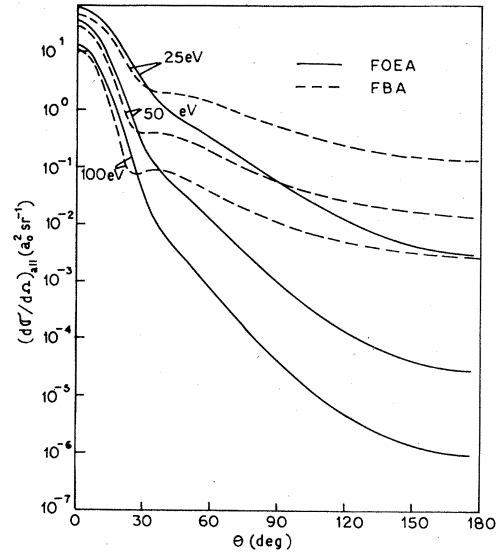


FIG. 2. Differential cross sections in units of a_0^2/sr for the Ps formation into all bound states of the positronium atom at $E=25, 50,$ and 100 eV.

Figure 2 represents the DCS for the Ps formation into all bound states of the positronium atom at $E=25, 50,$ and 100 eV. In obtaining these results we use the following relation:

$$\left(\frac{d\sigma}{d\Omega}\right)_{\text{all}} = \sum_{n=1}^5 \sum_{l=0}^{n-1} \frac{d\sigma_{nl}}{d\Omega} + \sum_{n=6}^{\infty} n^{-3} \sum_{l=0}^4 \prod_{r=0}^l \left[1 - \frac{r^2}{n^2}\right] \times \left[n_1^3 \frac{d\sigma_{n_1 l}}{d\Omega}\right]_{n_1 \rightarrow \infty}. \quad (31)$$

TABLE I. The total Ps-formation cross sections (πa_0^2) into different angular momentum states. Exponents of multiplication factors of 10 are indicated by superscripts.

n	l	E (eV)											
		20		40		100		200		300			
		a	b	a	b	a	b	a	b	a	b		
1	0	3.342	3.384	0.847	0.959	0.458^{-1}	0.611^{-1}	0.251^{-2}	0.383^{-2}	0.368^{-3}	0.605^{-3}		
2	0	0.228	0.243	0.112	0.127	0.687^{-2}	0.905^{-2}	0.361^{-3}	0.547^{-3}	0.513^{-4}	0.840^{-4}		
	1	0.222	0.113	0.570^{-1}	0.401^{-1}	0.186^{-2}	0.185^{-2}	0.526^{-4}	0.651^{-4}	0.505^{-5}	0.712^{-5}		
3	0	0.549^{-1}	0.593^{-1}	0.331^{-1}	0.377^{-1}	0.211^{-2}	0.277^{-2}	0.110^{-3}	0.166^{-3}	0.155^{-4}	0.254^{-4}		
	1	0.660^{-1}	0.324^{-1}	0.191^{-1}	0.131^{-1}	0.662^{-3}	0.657^{-3}	0.188^{-4}	0.233^{-4}	0.180^{-5}	0.254^{-5}		
	2	0.562^{-2}	0.443^{-2}	0.124^{-2}	0.955^{-3}	0.262^{-4}	0.241^{-4}	0.422^{-6}	0.451^{-6}	0.279^{-7}	0.334^{-7}		
4	0	0.213^{-1}	0.231^{-1}	0.139^{-1}	0.159^{-1}	0.899^{-3}	0.118^{-2}	0.468^{-4}	0.707^{-4}	0.659^{-5}	0.108^{-4}		
	1	0.276^{-1}	0.134^{-1}	0.838^{-2}	0.568^{-2}	0.296^{-3}	0.293^{-3}	0.842^{-5}	0.104^{-4}	0.806^{-6}	0.113^{-5}		
	2	0.313^{-2}	0.248^{-2}	0.727^{-3}	0.533^{-3}	0.157^{-4}	0.144^{-4}	0.254^{-6}	0.271^{-6}	0.169^{-7}	0.201^{-7}		
	3	0.704^{-4}	0.659^{-4}	0.141^{-4}	0.125^{-4}	0.205^{-6}	0.194^{-6}	0.194^{-8}	0.197^{-8}	0.895^{-10}	0.973^{-10}		

^aFirst Born approximation.

^bFirst-order exchange approximation.

We have restricted the value of l such that $l \leq 4$ since the contributions of the higher angular momentum states to the sum are negligible. It is evident from the figure that the contributions from the higher excited states strikingly improve the shape of the curve (see also Fig. 1), particularly near the cross-section minima. A similar prescription for the p -H system¹¹ yield results which are in good agreement with the available experimental findings.

B. Total cross sections

Our computed results for the integrated Ps-formation cross sections into different angular momentum states for some low-lying discrete states ($n=1-4$) at various incident positron energies are shown in Table I. For $l=0$ states FOEA results are always greater than those of the FBA. As E increases the percentage difference between these two sets of results increases. It is to be mentioned that at $E=25$ eV the contribution from the amplitude g^{FBA} and $(\mathcal{K}\mu_f/2\pi)$ for the s state are nearly equal at large angles whereas at $\theta=0^\circ$ the magnitude of the g^{FBA} is 13% larger than that of $(\mathcal{K}\mu_f/2\pi)$; both having the same sign. The FOEA amplitude being the sum of these two terms gets more contribution in the forward direction and consequently it enhances the DCS in the forward direction. This may be due to the fact that in the FOEA the contribution of the additional term U_i , an average interacting potential that mimics the short-range forces, dominates the s wave considerably. As E increases the percentage difference between the FBA and FOEA results for excited state Ps formation increases. As an example, for $8s$ states at $E=20$ eV their difference is $\sim 8\%$ whereas at $E=300$ eV it is almost 39%.

For the $l=1$ state except at low energies ($E \leq 100$ eV) the FOEA results overestimate their FBA counterparts. At low energies for the $l=1$ and $m=0$ state we noticed that the g^{FBA} amplitude changes sign twice while $(\mathcal{K}\mu_f/2\pi)$ changes sign only once throughout the energy range considered. The angular position (θ_0) at which this

change occurs is quite different in both the amplitudes. As a result this minimum shifts considerably in the FOEA amplitude. It is interesting to note that the maximum contribution to the integrated cross sections come from the range $0-\theta_0$ of the scattering angle. The contributions from the $l=1$ and $m=\pm 1$ states' amplitudes are very small, in that in the forward direction they have zero contributions, compared to the $l=1$ and $m=0$ states; the contribution of both the g^{FBA} and $(\mathcal{K}\mu_f/2\pi)$ are opposite in sign and consequently the FOEA amplitude becomes much smaller compared to the FBA amplitude.

In Table II we show the sum of the contributions from different angular momentum (l, m) states to the total Ps-formation cross sections into higher excited states at $E=20-1000$ eV. As the formation cross sections drop off rapidly with the rise of l values, we retain the value of l up to 4 throughout our discussion. The discrete-state ($n=1-16$) results in both the approximations being calculated using relations (14) and (20) whereas the asymptotic results as $n \rightarrow \infty$ are obtained employing the limiting expression given by Eq. (29).

As mentioned already, we have noted that at moderate or high incident energies, apart from a factor $n^{-3}[\prod_{r=0}^l(1-r^2n^{-2})]$ the cross section remains more or less unchanged with the increase of n . As a consequence, the asymptotic n^3 cross section $[n^3\sigma_{nl}]_{n \rightarrow \infty}$ for a particular angular momentum state if multiplied by the factor $\prod_{r=0}^l(1-r^2n^{-2})$ gives a good estimate of the n^3 cross sections for Ps formation into the corresponding n, l state provided the value of the principal quantum number n is not too small. The scaling law reads as

$$n^3\sigma_{nl} = \prod_{r=0}^l (1-r^2n^{-2}) [n^3\sigma_{n,l}]_{n \rightarrow \infty} \quad (32)$$

In order to use the above relation a knowledge of the asymptotic n^3 cross section is essential. We tabulate $[n^3\sigma_{nl}]_{n \rightarrow \infty}$ in Table III at various incident positron energies ranging from $E=20$ to 1000 eV.

TABLE II. Total n^3 Ps-formation cross sections (πa_0^2).

E (eV)	n	1	2	3	4	8	10	12	14	16	∞	Exp. ^c
20.0	a	3.342	3.602	3.417	3.334	3.252	3.241	3.235	3.232	3.229	3.222	
	b	3.385	2.843	2.595	2.502	2.412	2.401	2.395	2.391	2.388	2.381	
30.0	a	1.648	2.389	2.471	2.493	2.510	2.512	2.513	2.514	2.514	2.516	
	b	1.781	2.178	2.188	2.185	2.179	2.178	2.177	2.177	2.177	2.176	
50.0	a	0.464	0.759	0.823	0.845	0.867	0.870	0.872	0.872	0.873	0.875	
	b	0.545	0.797	0.847	0.865	0.882	0.884	0.885	0.885	0.886	0.887	
100.0	a	0.458	0.698	0.754	0.775	0.796	0.798	0.800	0.800	0.801	0.803	1
	b	0.611	0.872	0.931	0.952	0.974	0.976	0.978	0.978	0.979	0.981	1
200.0	a	0.251	0.331	0.348	0.355	0.361	0.362	0.362	0.363	0.363	0.363	2
	b	0.383	0.489	0.512	0.521	0.529	0.530	0.530	0.531	0.531	0.532	2
500.0	a	0.275	0.314	0.322	0.325	0.328	0.328	0.328	0.328	0.328	0.329	4
	b	0.491	0.557	0.571	0.575	0.580	0.581	0.581	0.581	0.581	0.582	4
1000.0	a	0.317	0.347	0.353	0.356	0.358	0.358	0.358	0.358	0.358	0.358	5
	b	0.591	0.648	0.659	0.663	0.667	0.668	0.668	0.668	0.668	0.668	5

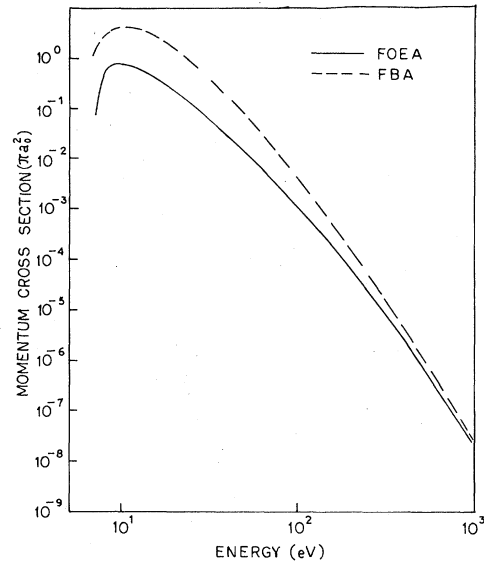
^aFirst Born approximation.

^bFirst-order exchange approximation.

^cThe integer in this column is the inverse power of 10 to be multiplied with the numbers in the corresponding row.

TABLE III. n^3 times the asymptotic ($n \rightarrow \infty$) Ps-formation cross sections (in πa_0^2). Exponents of multiplication factors of 10 are indicated by superscripts.

l	E (eV)										
	20.0	25.0	40.0	50.0	100.0	200.0	300.0	400.0	500.0	1000.0	
0	a	1.2181	1.4739	0.8904	0.5417	0.5844 ⁻¹	0.3031 ⁻²	0.4259 ⁻³	0.9823 ⁻⁴	0.3042 ⁻⁴	0.6923 ⁻⁶
	b	1.3257	1.6311	1.0168	0.6340	0.7661 ⁻¹	0.4575 ⁻²	0.6967 ⁻³	0.1690 ⁻³	0.5416 ⁻⁴	0.1322 ⁻⁵
1	a	1.7319	1.3624	0.5591	0.3005	0.2036 ⁻¹	0.5797 ⁻³	0.5542 ⁻⁴	0.9644 ⁻⁵	0.2393 ⁻⁵	0.2710 ⁻⁷
	b	0.8379	0.6717	0.3742	0.2272	0.2011 ⁻¹	0.7158 ⁻³	0.7796 ⁻⁴	0.1484 ⁻⁴	0.3932 ⁻⁵	0.5243 ⁻⁷
2	a	0.2587	0.1871	0.6376 ⁻¹	0.3138 ⁻¹	0.1430 ⁻²	0.2328 ⁻⁴	0.1539 ⁻⁵	0.2039 ⁻⁴	0.4077 ⁻⁷	0.2328 ⁻⁹
	b	0.2052	0.1369	0.4793 ⁻¹	0.2488 ⁻¹	0.1310 ⁻²	0.2480 ⁻⁴	0.1838 ⁻⁵	0.2676 ⁻⁶	0.5780 ⁻⁷	0.4152 ⁻⁹
3	a	0.1299 ⁻¹	0.8843 ⁻²	0.2756 ⁻²	0.1295 ⁻²	0.4227 ⁻⁴	0.4040 ⁻⁶	0.1865 ⁻⁷	0.1892 ⁻⁸	0.3062 ⁻⁹	0.8907 ⁻¹²
	b	0.1219 ⁻¹	0.7942 ⁻²	0.2431 ⁻²	0.1162 ⁻²	0.3997 ⁻⁴	0.4088 ⁻⁶	0.2027 ⁻⁷	0.2210 ⁻⁸	0.3830 ⁻⁹	0.1431 ⁻¹¹

^aFirst Born approximation.^bFirst-order exchange approximation.FIG. 3. Momentum-transfer cross sections in units of πa_0^2 for the Ps formation in the ground state.

C. Momentum-transfer cross sections

The MTCS provides an even more stringent test of the models. Since the MTCS is a weighted integral of the DCS which deemphasizes small-angle scattering, it is expected that the cross section would be much more sensitive to the short-range interaction. Figure 3 represents the ground-state MTCS as a function of the incident positron energy in the FBA and the FOEA. Throughout the energy range considered the FBA values remain much higher than their FOEA counterpart. This may be attributed to the fact that the elastic MTCS are very sensitive to the large-angle scattering; the FBA amplitudes in that region are much higher than those of the FOEA. We notice that the same feature is shown by the result for Ps formation into $n=2$ states.

VI. CONCLUSION

In the present study we employed a class of first-order approximation theory, namely the FBA and the FOEA, to investigate the Ps formation into arbitrary excited states in $e^- + H(1,0,0)$ scattering. Previously, the Ps-formation cross sections in the FOEA were available only for the $1s$ state. We have compared the results as obtained in the FBA and FOEA for Ps formation into various excited levels.

The angular distributions in the FBA for s states ($l=0$) show a zero at some scattering angle and it moves towards the forward direction as the value of E increases. The zero position of the angular distribution does not, however, depend on the value of n in that for any excited states it remains almost the same. At $E < 200$ eV the FOEA results exhibit a zero in the DCS for s -state Ps formation, but from our observations at $E=200, 500,$ and 1000 eV we find no such zero or minimum in the angular distributions. For higher angular momentum states ($l \geq 1$) the

angular distributions do not predict the existence of such a zero either in the FBA or in the FOEA.

We have also presented the results for DCS for Ps formation into all possible bound states using the scaling law. However, as of now there are no experimental results for a comparison. As already mentioned, we have reproduced the results previously reported in Refs. 9 and 10. In the present study the minimum projectile energy considered is 20 eV. However, the earlier observation of Mandal and Guha has shown that at low energies the FOEA results for the ground-state Ps formation are lower than the corresponding FBA values. This is in agreement with the rigorous results on the Ps formation obtained by the low energy *s*- and *p*-wave calculations¹² for Ps formation in the *1s* state. These calculations predict that at low energies the Ps-formation cross sections are considerably lower than the FBA results. The FOEA is expected to yield results much better than their FBA counterpart since the FOEA rectifies some of the inadequacies encountered in the FBA and, moreover, the FOEA accounts

for a certain amount of distortion owing to the presence of the distorting potential V_D in the interaction.

The formation cross sections into highly excited states do satisfy the n^{-3} law irrespective of the incident energy. At high incident energies the Ps-formation cross sections are larger than the FBA results. Even at $E=1$ keV the ground-state Ps-formation cross sections in the FOEA do not agree with the FBA results; their difference is $\sim 5\%$. The use of the asymptotic ($n \gg 1$) cross sections in estimating the discrete-state results with the help of the "scaling law" [see Eq. (32)] is discussed. The momentum-transfer cross sections that are essential for the analysis of the results of the swarm experiments are also presented.

ACKNOWLEDGMENT

The authors are most grateful to Professor N. C. Sil for his valuable comments and suggestions.

¹E. L. Chupp, D. J. Forrest, and A. N. Suri, Proceedings of the IAU COSPAR Symposium No. 68 Solar Gamma-, X-, and XUV Radiations, edited by Kane (Reidel, Dordrecht, 1975), p. 431; E. L. Chupp, D. J. Forrest, P. R. Higbie, A. N. Suri, C. Tsai, and P. P. Dunphy, *Nature (London)* **241**, 333 (1973).

²M. Leventhal, C. J. McCallum, and P. D. Stang, *Astrophys. J.* **225**, L11 (1978).

³R. Ramaty, B. Kozlovsky, and R. E. Lingenfelter, *Space Sci. Rev.* **18**, 341 (1975); C. J. Crannell, G. Joyce, R. Ramaty, and C. Wernitz, *Astrophys. J.* **210**, 582 (1976); R. W. Bussard, R. Ramaty, and R. J. Drachman, *ibid.* **228**, 928 (1979); see also T. S. Stein and E. W. Kauppila, *Advances in Atomic and Molecular Physics* (Academic, New York, 1983), Vol. 18, p. 53.

⁴M. Charlton, G. Clark, T. C. Griffith, and G. R. Heyland, *J. Phys. B* **16**, L465 (1983).

⁵E. Feenberg, *Phys. Rev.* **40**, 60 (1932). See also B. H.

Bransden, *Advances in Atomic and Molecular Physics* (Academic, New York, 1965), Vol. 1, p. 85.

⁶K. L. Bell and B. L. Moiseiwitsch, *Proc. Roy. Soc. London, Ser. A* **276**, 346 (1963).

⁷B. C. Saha, H. P. Saha, and N. C. Sil, *J. Phys. Soc. Jpn.* **47**, 1634 (1979); *Indian J. Phys.* **55B**, 16 (1981); see also B. L. Moiseiwitsch and S. J. Smith, *Rev. Mod. Phys.* **40**, 238 (1968).

⁸P. K. Roy, B. C. Saha, and N. C. Sil, *J. Phys. B* **13**, 3401 (1980).

⁹N. C. Sil, B. C. Saha, H. P. Saha, and P. Mandal, *Phys. Rev. A* **19**, 655 (1979).

¹⁰P. Mandal and S. Guha, *J. Phys. B* **12**, 1603 (1979).

¹¹P. K. Roy, B. C. Saha, and N. C. Sil, *Indian J. Phys.* **56B**, 199 (1982).

¹²Y. F. Chan and P. A. Fraser, *J. Phys. B* **6**, 2504 (1973); Y. F. Chan and R. P. McEachran, *ibid.* **9**, 2869 (1976); J. W. Hummerston, *Can. J. Phys.* **60**, 591 (1982).